RAPID COMMUNICATIONS

PHYSICAL REVIEW B VOLUME 61, NUMBER 4 15 JANUARY 2000-II

Resonant elastic x-ray scattering of graphite and diamond at the carbon *K* threshold

Yasuji Muramatsu
NTT Lifestyle and Environmental Technology Laboratories, Musashino-shi, Tokyo 180-8585, Japan

Melissa M. Grush
University of Tennessee, Knoxville, Tennessee 37996

Rupert C. C. Perera
Center for X-Ray Optics, Lawrence Berkeley National Laboratory, Berkeley, California 94720

(Received 26 May 1999; revised manuscript received 11 November 1999)

Resonant elastic x-ray scattering (REXS) was observed at the carbon *K* threshold of graphite powder, and a small amount of excitonic x-ray scattering was observed in diamond. A comparison of the energy spectra of REXS in graphite with the carbon *K* x-ray absorption spectra, and with the calculated energy spectra of the unoccupied density of states, suggests that REXS is caused by the transition of the ''participator'' electrons via $p\pi^*$ states in sp^2-carbon atoms. The probabilities of transition to ''participator'' REXS or to ''spectator'' resonant inelastic x-ray scattering in the resonant radiative-decay process of graphite powder, were determined from REXS spectroscopy to be approximately 47% and 53%, respectively.

Soft x-ray emission spectroscopy (SXES), using highly brilliant monochromatized synchrotron radiation as an excitation source, has become a key spectroscopic method for materials science because it is a powerful tool for analyzing the electronic structure of materials in relation to their band structure.[1] In addition, the resonant phenomena observed in the excitation near the threshold provide information about the radiative-decay process during inner-shell excitation that cannot be obtained using other methods. This has stimulated many researchers to try to comprehensively understand the decay processes and electronic structures of materials and to explore new fields in materials science.

The resonant radiative-decay process can in general be divided into two types. One is resonant *inelastic* x-ray scattering (RIXS), caused by the interaction of ''spectator'' electrons, excited in threshold localized states, with valence electrons; the other is resonant *elastic* x-ray scattering (REXS), caused by the radiative transition of ''participator'' electrons to the inner core-holes. Spectator RIXS has been intensively studied by many researchers, and interesting phenomena related to the resonant radiative-decay process have been observed in many materials.[2,3] In comparison, the study of participator REXS is less advanced; REXS has been clearly observed only in boron compounds.[4–6] However, it should be possible to observe participator REXS in other compounds, and this would provide information about their resonant radiative-decay process and electronic structure, complementing the RIXS information.

We have studied participator REXS to gain a comprehensive understanding of the resonant radiative-decay process. We focused on graphite and diamond because the electronic structures and RIXS of these carbon materials[7,8] and the angular resolved SXES of graphite[9] have already been well investigated. In this paper, we describe our elastic x-ray scattering measurements of graphite and diamond at the carbon *K* threshold, and discuss REXS in these carbon materials in relation to the electronic structure characterized by sp^2- and sp^3-carbon atoms.

REXS experiments have measured the energy-dependent spectra of elastic x-ray scattering at the threshold. It is well known that both the energy spectra of carbon *K* x-ray emission and the inelastic x-ray scattering of graphite depend on the angle of detection relative to the crystal-structure axis.[9] We therefore used a sample of graphite powder, in which the average particle size was 45 μm, for our REXS measurements to average out this detection-angle dependence in the elastic x-ray scattering measurements. A bulk sample of diamond ($4\times4\times1\ \text{mm}^3$) was also used for the measurements. The spectral measurements were carried out by using a grating x-ray spectrometer with a position-sensitive detector (PSD) installed in beamline (BL) 8.0 (Ref. 10) at the Advanced Light Source (ALS). Figure 1 shows the top view of the optical arrangement for the measurements. Monochromatized undulator beams irradiate a sample, and fluorescent x rays and scattered x rays emitted from the sample are monochromatized by a spherical grating and detected by the PSD.

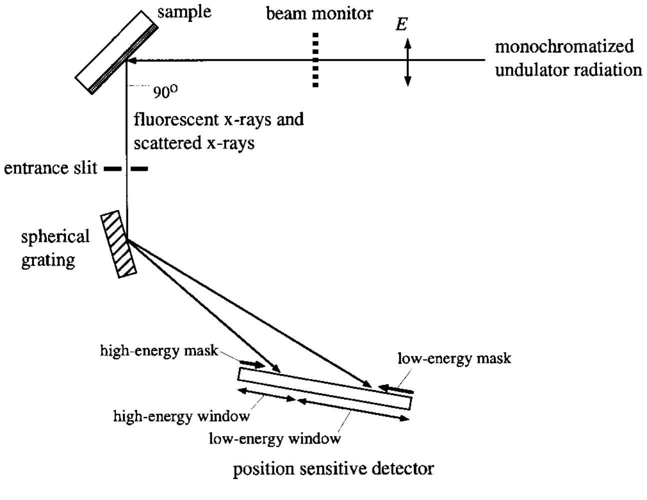

FIG. 1. Top view of the optical arrangement for the elastic x-ray scattering measurements in BL-8.0.

The entrance slit and the grating of the grating x-ray spectrometer are aligned perpendicularly to the incident undulator beams in the horizontal *E*-vector plane. The energy resolution (ΔE) of the grating x-ray spectrometer was estimated to be less than 1 eV in the carbon *K* region for a 100-μm entrance slit and a 600-line/mm grating whose curvature had a 10-m radius. To measure the energy-dependent spectra of elastic x-ray scattering, we measured the partial-fluorescence-yield (PFY) absorption spectra using three different PSD window widths optimized by the high- and low-energy masks of the PSD. In the PSD positioned to detect carbon *K* x-ray emission arising from the x-ray excitation near the carbon *K* threshold, RIXS or fluorescent *K-V* x-ray emission can be detected in the lower energy region and elastic x-ray scattering can be detected in the higher energy region. We can therefore obtain the energy-dependent spectra of the elastic x-ray scattering from the PFY-absorption measurements by monitoring the x-ray intensity in the high-energy window of the PSD. The energy resolution in the PFY-absorption measurements was estimated to be less than 0.5 eV for a 100-μm exit slit and a 380-line/mm grating with a 70-m radius in the beamline monochromator. The total-electron-yield (TEY) absorption spectra were also measured by monitoring the sample photocurrent in BL-6.3.2.[11] The energy resolution in the TEY-absorption measurements was estimated to be 0.07 eV for a 20-μm exit slit and a 600-line/mm grating.

Figure 2 shows the carbon *K* x-ray emission spectra (upper panels) and PFY- and TEY-absorption spectra (lower panels) of (a) graphite powder and (b) diamond. The carbon *K* x-ray emission spectra were obtained using 320-eV x-ray excitation. For graphite, the PSD was positioned to detect x rays from 263 to 298 eV as shown in the carbon *K* x-ray emission spectrum. In the x-ray emission spectrum, elastic x-ray scattering can be expected in the energy region above 284 eV and RIXS or fluorescent *K-V* x-ray emission can be expected below 284 eV. In this PSD setup, the width of the wide window (denoted by *A* in the figure) was tuned from 263 to 298 eV, that of the low-energy window (*B*) was from 263 to 284 eV, and that of the high-energy window (*C*) was from 284 to 298 eV, as illustrated in the x-ray emission spectrum. The lower panel shows the PFY-absorption spectra taken with (*A*) wide, (*B*) low-energy, and (*C*) high-energy windows, as well as the spectra obtained after subtracting (*B*) from (*A*) and the TEY-absorption spectra of graphite. These PFY-absorption spectra can be obtained by monitoring I/I_0, where *I* is the x-ray intensity measured by the PSD, and I_0 is the incident-beam photocurrent intensity measured by a gold-mesh beam monitor in front of the samples. In these measurements, the shape of the I/I_0 spectra may not precisely reflect the carbon *K* absorption structure of the samples because of carbon contamination of the beamline optics in BL-8.0. Therefore, the spectra of *I* and I_0 are shown as part of the high-energy-window spectrum (*C*) to clarify the carbon contamination effects on I_0; a dip structure was observed at 284 eV in the I_0 spectrum. This shows that the peak structure observed at 284 eV in the I/I_0 spectra, which is denoted by an asterisk in the figure, is affected by the carbon contamination.

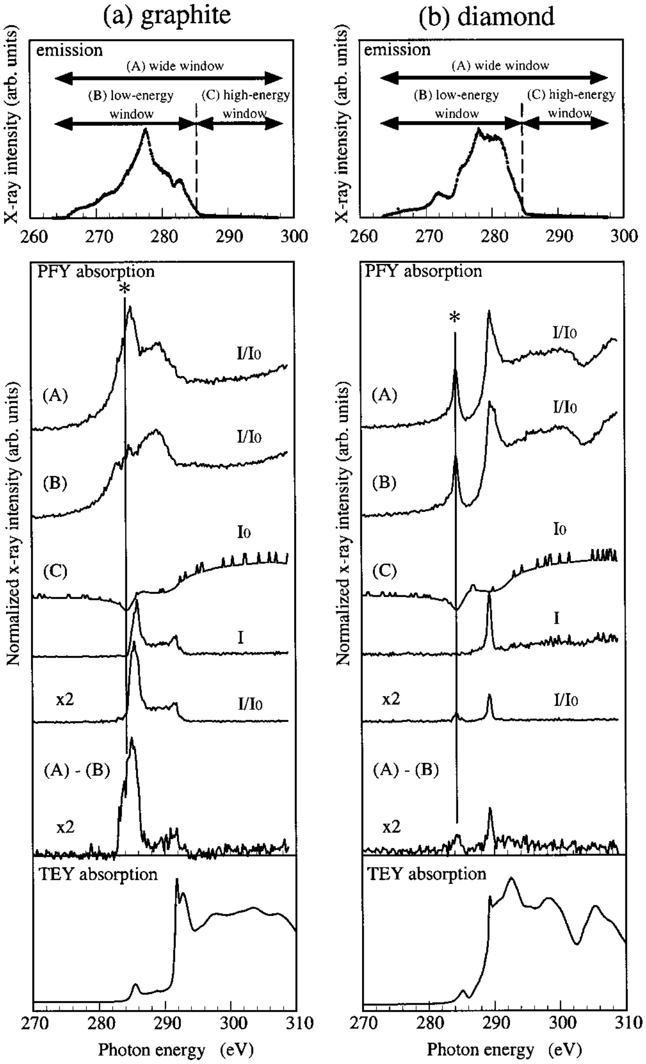

FIG. 2. Carbon *K* x-ray emission spectra (upper panels) and partial-fluorescence-yield (PFY) and total-electron-yield (TEY) absorption spectra (lower panels) of (a) graphite powder and (b) diamond. The carbon *K* x-ray emission spectra were obtained using 320-eV excitation. The PFY absorption spectra were taken by monitoring the x-ray intensity measured by the PSD with (*A*) wide, (*B*) low-energy, and (*C*) high-energy windows. Spectra obtained after subtracting (*B*) from (*A*), denoted by $(A)-(B)$, and the total-electron-yield (TEY) absorption spectra are also shown. The peak structure observed at 284 eV in the I/I_0 spectra, which is affected by carbon contamination of the beamline optics, is denoted by an asterisk.

We detected RIXS in the low-energy window (*B*), elastic x-ray scattering in the high-energy window (*C*), and both RIXS and elastic x-ray scattering in the wide window (*A*). Therefore, energy-dependent spectra of elastic x-ray scattering can be obtained from the PFY-absorption spectra of (*C*) or the spectra obtained after subtracting (*B*) from (*A*). In the high-energy window, PFY-absorption spectrum of the graphite (*C*), a sharp peak was observed near 285 eV, followed by a slight plateau in the energy region from 285 to 292 eV. These spectral features of (*C*) were approximately reproduced in the spectrum obtained after subtracting (*B*) from (*A*). Comparing these energy-dependent spectra of elastic x-ray scattering with the TEY-absorption spectrum, we found that the sharp 285-eV scattering peak corresponds to the π^*-absorption peak and that the broad portion in the

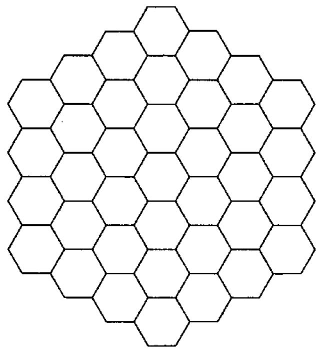

(a) Cluster model, $C_{96}H_{24}$

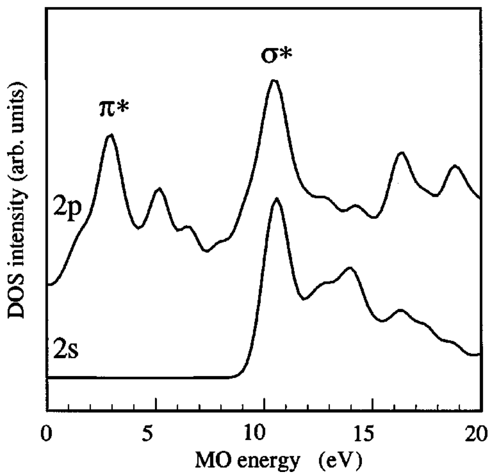

(b) DOS spectra

FIG. 3. (a) Cluster model of $C_{96}H_{24}$ used in the DV-$X\alpha$ calculations of graphite; (b) calculated unoccupied $2p$- and $2s$-DOS spectra of the cluster model. The DOS spectra were obtained by convoluting the 0.5-eV-wide Lorentzian functions on the individual DOS.

range from 285 to 292 eV corresponds to the region between the π^*- and σ^*-absorption peaks. No scattering structure was observed above the σ^*-peak region. Although the low-energy tail of the 285-eV scattering peak in the spectrum obtained after subtracting (*B*) from (*A*) is partially observed in the 284-eV region in which the peak structure of carbon contamination effects should be observed, the main spectral features of the elastic x-ray scattering are hardly affected by the carbon contamination effects. This elastic x-ray scattering in graphite thus corresponds to the threshold unoccupied electronic structure, and it can be identified as REXS.

For diamond, shown in Fig. 2(b), a peak at 289 eV and a small peak at 284 eV were observed in the high-energy window PFY-absorption spectrum (*C*) and the spectrum obtained after subtracting (*B*) from (*A*). In comparison to the I_0 spectrum shown in (*C*), it is clear that the 284-eV peaks denoted by an asterisk in the I/I_0 spectra of (*A*), (*B*), and (*C*), and in the spectrum obtained after subtracting (*B*) from (*A*) are the result of carbon contamination of the beamline optics, as mentioned above for graphite. The peak at 289 eV, however, corresponds to the threshold peak caused by an exciton in the TEY absorption. Therefore, the 289-eV peak may also be elastic x-ray scattering via exciton states. This resonant phenomenon in exciton states was discovered and explained by Ma *et al.*[12] as resulting from the vibronic coupling effects of core excitons. Except for this excitonic x-ray scattering, no significant scattering structure was observed for diamond.

To describe the spectral features of REXS in graphite, we calculated the unoccupied density of states (DOS) of graphite by using discrete-variational (DV)-$X\alpha$ molecular orbital calculation.[13] Figure 3(a) shows the cluster model of $C_{96}H_{24}$ we used for the DV-$X\alpha$ calculations, and Fig. 3(b) shows the calculated unoccupied $2p$- and $2s$-DOS spectra of the cluster model. The DOS spectra were obtained by convoluting the 0.5-eV-wide Lorentzian functions on the individual DOS. The $2p$-DOS is widely spread in the molecular-orbital (MO) energy region of 1 to 20 eV. The peaks at 2 and 10 eV can be assigned to π^* and σ^*, respectively. The energy gap of 7 eV between these calculated π^* and σ^* peaks approximates that between the peaks measured at 285 and 292 eV. In comparison, the $2s$ DOS exists only above an MO energy level of 9 eV. This indicates that the region between the π^* and σ^* peaks is composed of only $p\pi^*$ states. As shown in Fig. 2(a), REXS was observed in the region between the π^* and σ^* peaks. From this we conclude that REXS occurs via the unoccupied $p\pi^*$ states ($1s$-$p\pi^*$-$1s^{-1}$ transition) in sp^2-carbon atoms. This REXS transition via $p\pi^*$ states agrees with the intense REXS observed in triangularly coordinated boron compounds.[4,5] In diamond, no significant REXS was observed, except for the excitonic x-ray scattering peak at 289 eV. This agrees with the above-mentioned REXS mechanism, because there are no $p\pi^*$ states in the sp^3-carbon atoms of diamond. This suggests that we may experimentally distinguish the $p\pi^*$ states from the complicated hybridized electronic structure in the unoccupied states of carbon compounds by using REXS spectroscopy.

Figure 4 overlays the PFY-absorption spectrum of the graphite powder taken with the wide window (*A*) onto that

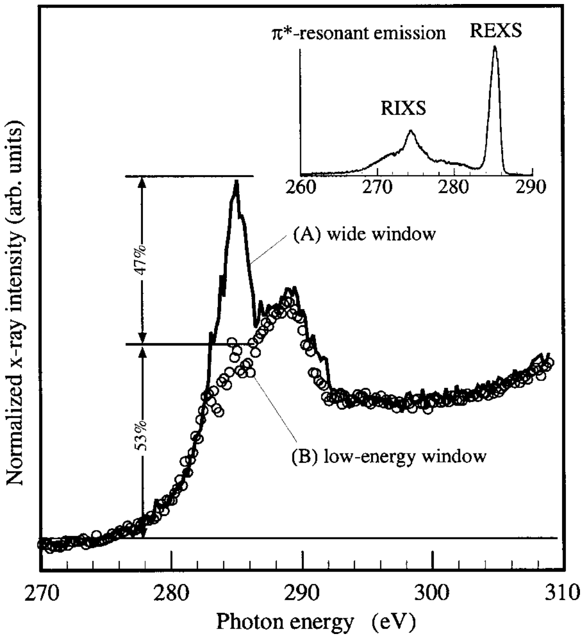

FIG. 4. Comparison of peak heights between PFY-absorption spectra of graphite powder taken with (*A*) the wide window (solid line) and (*B*) the low-energy window (open circles). The inset shows the π^*-resonant carbon *K* x-ray emission spectrum of the graphite powder.

taken with the low-energy window (*B*), with the x-ray scattering intensities normalized. The spectral height at 285 eV in the low-energy-window spectrum shows the probability of spectator RIXS occurring. In comparison, the peak height at 285 eV in the wide-window spectrum includes both spectator RIXS and participator REXS. Consequently, we can quantitatively determine the transition-probability ratio of spectator RIXS and participator REXS by comparing these peak heights; the probabilities of transition to participator REXS or to spectator RIXS in the π^*-resonant radiative-decay process of graphite powder were determined to be approximately 47% and 53%, respectively. This ratio corresponds to the peak area ratio between the REXS and RIXS peaks in the π^*-resonant carbon *K* x-ray emission spectrum in the inset in the figure.

In conclusion, we have observed strong REXS at the carbon *K* threshold of graphite powder. The energy region of the REXS corresponded to that of the $p\pi^*$ states of graphite. The REXS is caused by the transition of the participator electrons via $p\pi^*$ states in sp^2-carbon atoms. In diamond, however, there are no $p\pi^*$ states, and no REXS was observed, except for a small amount of excitonic x-ray scattering. This shows that REXS spectroscopy may identify the $p\pi^*$ orbitals in the unoccupied hybridized orbitals of carbon atoms. The transition probability ratio between participator REXS and spectator RIXS in the resonant radiative-decay process can be determined from REXS spectroscopy. In graphite powder, the probabilities of transition to REXS and to RIXS were measured and found to be approximately 47% and 53%, respectively. This shows that REXS spectroscopy at the thresholds of inner-shell excitation provides information about the electronic structures of unoccupied orbitals and about the resonant radiative-decay process, complementing RIXS spectroscopy.

We wish to express thanks to Professor Thomas A. Callcott of the University of Tennessee and to Dr. Eric M. Gullikson and Dr. James H. Underwood of Lawrence Berkeley National Laboratory for their helpful support in the spectroscopic measurements at ALS. We are also grateful to Dr. Eric L. Shirley of the National Institute of Standards and Technology, and to Dr. Takayoshi Hayashi of NTT Lifestyle and Environmental Technology Laboratories for their helpful discussions.

---

[1] J. Nordgren, in *New Directions in Research with Third-Generation Soft X-ray Synchrotron Radiation Sources*, edited by A. S. Schlachter and F. J. Wuilleumier (Kluwer Academic Publishers, Dordrecht, 1994), p. 189; D. L. Ederer, K. E. Miyano, W. L. O'Brien, T. A. Callcott, Q.-Y. Dong, J. J. Jia, D. R. Mueller, J.-E. Rubensson, R. C. C. Perera, and R. Shuker, *ibid.*, p. 281.

[2] *Raman Emission by X-Ray Scattering*, edited by D. L. Ederer and J. H. McGuire (World Scientific, Singapore, 1996).

[3] *Resonant Inelastic Soft X-ray Scattering (RIXS)*, edited by W. Eberhardt, J. Luning, and J.-E. Rubensson, special issue of Appl. Phys. A: Mater. Sci. Process. **65A** (1997).

[4] Y. Muramatsu, M. Oshima, and H. Kato, Phys. Rev. Lett. **71**, 448 (1993).

[5] Y. Muramatsu, J. Kawai, T. Scimeca, M. Oshima, and H. Kato, Phys. Scr. **50**, 25 (1994).

[6] J. A. Carlisle, L. J. Terminello, E. A. Hudson, R. C. C. Perera, J. H. Underwood, T. A. Callcott, J. J. Jia, D. L. Ederer, F. J. Himpsel, and M. G. Samant, Appl. Phys. Lett. **67**, 34 (1995).

[7] J. A. Carlisle, E. L. Shirley, E. A. Hudson, L. J. Terminello, T. A. Callcott, J. J. Jia, D. L. Ederer, R. C. C. Perera, and F. J. Himpsel, Phys. Rev. Lett. **74**, 1234 (1995).

[8] Y. Ma, N. Wassdahl, P. Skytt, J. Guo, J. Nordgren, P. D. Johnson, J.-E. Rubensson, T. Boske, W. Eberhardt, and S. D. Kevan, Phys. Rev. Lett. **69**, 2598 (1992).

[9] P. Skytt, P. Glans, D. C. Mancini, J.-H. Guo, N. Wassdahl, J. Nordgren, and Y. Ma, Phys. Rev. B **50**, 10 457 (1994).

[10] J. J. Jia, T. A. Callcott, J. Yurkas, A. W. Ellis, F. J. Himpsel, M. G. Samant, J. Stohr, D. L. Ederer, J. A. Carlisle, E. A. Hudson, L. J. Terminello, D. K. Shuh, and R. C. C. Perera, Rev. Sci. Instrum. **66**, 1394 (1995).

[11] J. H. Underwood, E. M. Gullikson, M. Koike, P. J. Batson, P. E. Denham, K. D. Franck, R. E. Tackaberry, and W. F. Steele, Rev. Sci. Instrum. **67**, 3371 (1996).

[12] Y. Ma, P. Skytt, N. Wassdahl, P. Glans, D. C. Mancini, J. Guo, and J. Nordgren, Phys. Rev. Lett. **71**, 3725 (1993).

[13] C. Satoko, M. Tsukada, and H. Adachi, J. Phys. Soc. Jpn. **45**, 1333 (1978).